Dynamics of Anti-Proton – Protons and Anti-Proton – Nucleus Reactions

(Reported at International Workshop on Nuclear Theory IWNT-35, Rila 2016, Bulgaria)

A. Galoyan[1], A. Ribon[2], V. Uzhinsky[3]

A short review of simulation results of anti-proton-proton and anti-proton-nucleus interactions obtained with Geant4 FTF (Fritiof) model is presented. The model uses the main assumptions of the Quark-Gluon-String Model or Dual Parton Model. The model assumes production and fragmentation of quark-anti-quark and diquark-anti-diquark strings in the mentioned interactions. Key ingredients of the model are cross sections of string creation processes and an usage of the LUND string fragmentation algorithm. The determined cross sections and improvements of the algorithm allow to satisfactory describe a large set of experimental data, in particular, strange particle production, Λ hyperons and K mesons.

arXiv:1610.08341v2 [nucl-th] 28 Oct 2016

1 Introduction

Simulations of anti-proton and anti-nucleus interactions with protons and nuclei are needed for cosmic space experiments like PAMELA, BESS, AMS, CAPRISE and so on which are going to search for anti-nuclei in cosmic rays. They hope this will bring a new light on the question about anti-matter in our Universe. A detailed experimental study of anti-proton-proton and anti-proton-nucleus interactions is foreseen at the future FAIR facilities (GSI, Darmstadt, Germany) by the PANDA Collaboration. The accelerator experiments and the cosmic ray experiments need estimations of properties of the mentioned interactions ($\bar{p}A$, $\bar{A}A$) for reconstruction and identification of anti-nuclei and reaction products. This requires a computer code for a good simulation of the reactions. Recently, it becomes possible to simulate the interactions in the well-known Geant4 toolkit [1]. At a creation of the simulation code, we used the main assumptions of the Dual-Parton or Quark-Gluon-String model (DPM/QGSM) [2]. For calculations of anti-proton-nucleus cross sections, we used the Glauber approach [3, 4, 5]. An extension of DPM/QGSM for anti-proton-nucleus reactions was proposed also. The main simulation results and assumptions of the model well be presented below.

2 Main processes of $\bar{p}p$ interactions

Usually, the following list of diagrams shown in Fig. 1 is considered in high energy phenomenology for anti-proton-proton interactions. The diagram "a" corresponds to string junction's annihilation with 3 quark-anti-quark string's creation. The string junction is a gluonic object which couples together quarks in baryon. It is presented by dashed line in the figure. The diagram "b" represents quark and anti-quark annihilation leading to diquark-antidiquark string creation. The diagram "c" corresponds to quark-anti-quark and string junction's annihilations with creation of 2 quark-anti-quark strings. Diagrams "d" and "f" can be responsible for exotic meson production. The last diagrams at the bottom of the figure are important at high energies. They are connected with pomeron exchange in t-channel.

Energy dependencies of the cross sections of the processes in some cases are predicted by the reggeon phenomenology. They are also shown in the figure. An elaborated scheme for a calculation of the cross sections in the phenomenology was proposed in our papers [6, 7]. As was shown in the papers, the approach is valid at $P_{lab} > 3$ GeV/c. Because experimental studies require much less energies, we undertook a new attempt to estimate the cross sections. It is presented in the paper [8].

$$\sigma_a = 25/\sqrt{s-4m^2} \quad (mb), \tag{1}$$

$$\sigma_b = 15.65 + 700 \cdot (2.172 - \sqrt{s})^{2.5} \quad (mb), \quad \sqrt{s} \leq 2.172\ GeV, \tag{2}$$

$$\sigma_b = 34/\sqrt{s} \quad (mb), \quad \sqrt{s} > 2.172\ GeV, \tag{3}$$

[1]VBLHEP, JINR, Dubna 141980, Russia
[2]CERN, CH-1211 Geneva 23, Switzerland
[3]LIT, JINR, Dubna 141980, Russia

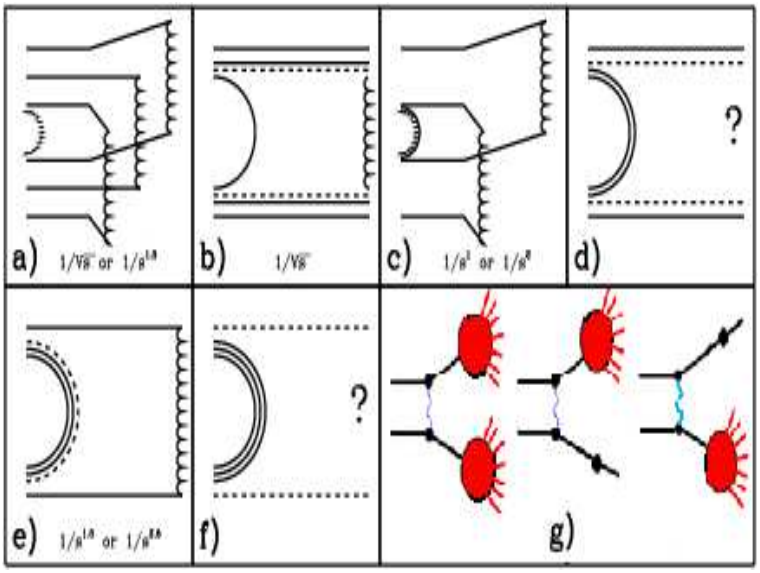

Figure 1: Quark flow diagrams of $\bar{p}p$ interactions.

$$\sigma_c = \frac{2}{\sqrt{s = 4m^2}} \left(\frac{m_p + m_t}{s} \right)^2 \quad (mb), \tag{4}$$

$$\sigma_e = 140/s \quad (mb), \tag{5}$$

Processes without annihilations dominate at high energies. They are presented in the bottom of Fig. 1. Their cross sections can be described by

$$\sigma_{FTF} = 35 \cdot (1 - 2.1/\sqrt{s}) \quad (mb). \tag{6}$$

For a fragmentation of the strings, we use the standard LUND fragmentation algorithm implemented in Geant4.

All of these allows to simulate the main channels of $\bar{p}p$ interactions (see Figs. 2 and 3).

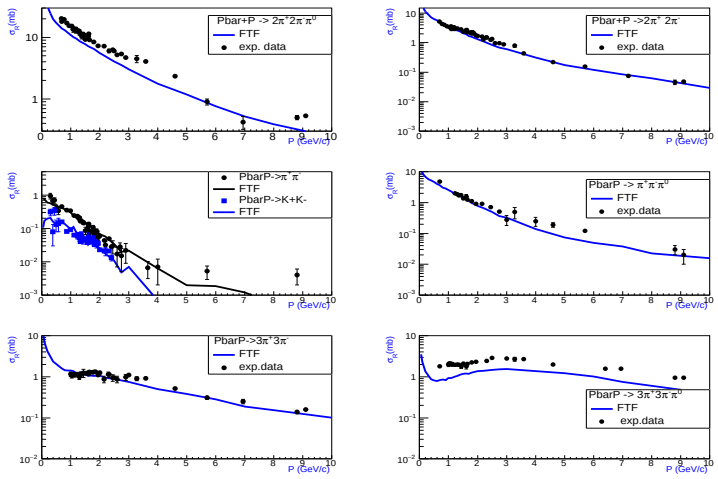

Figure 2: Cross sections of $\bar{p}p$ interactions with only mesons in final states. The points are experimental data. The lines are FTF model calculations.

As seen, the estimated cross sections, the improved string fragmentation algorithm and the FTF model of Geant4 allow to describe general properties of $\bar{p}p$ interactions. Thus, we conclude that the ex-

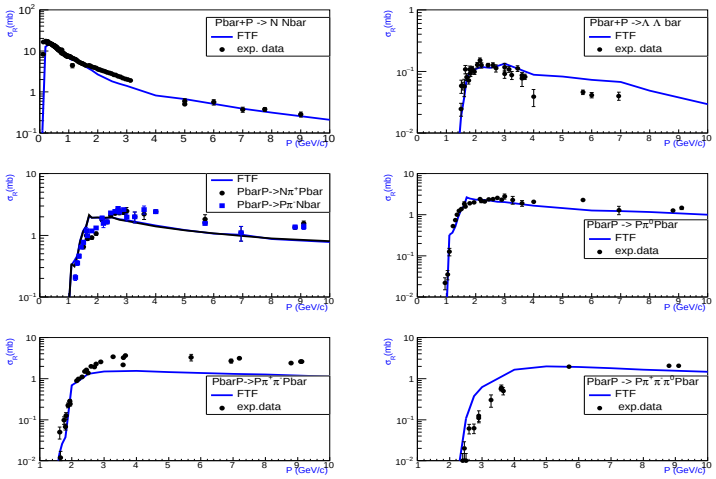

Figure 3: Cross sections of $\bar{p}p$ interactions with baryons in final states. The points are experimental data. The lines are FTF model calculations.

isting phenomenology of anti-baryon-baryon annihilation and hadron-nucleon high energy reactions with corresponding cross sections can be considered as a unified base for understanding of the $\bar{p}p$ interactions.

3 $\bar{p}A$ interactions

The first task in a simulation of the interactions is an estimation of anti-proton-nucleus and anti-nucleus-nucleus interaction cross sections (total, elastic and inelastic). It is natural to use the Glauber approach for calculations of the cross sections. For the first time, a good description of elastic anti-proton-deuteron scattering was reached in the classical paper by V. Franco and R.J. Glauber [9] in 1966. After that, in 1985 O.D. Dalkarov and V.A. Karmanov [10] showed that elastic and inelastic (with excitation of nuclear levels) anti-proton scattering on C, Ca, and Pb nuclei are described quite well at $\bar{p}$ kinetic energies of 46.8 and 179.7 MeV within the approximation. The Glauber approach in the question was also used in many other papers. We applied the approach in our paper [11] and obtained the results presented in Fig. 4. As seen, the agreement between the experimental data and the calculations is rather good. More details of the calculations and results are presented in [11]. A code for calculation of the total, elastic and inelastic cross sections of anti-protons and light anti-nuclei interactions with nuclei based on the Glauber approach is implemented in Geant4 toolkit. This code can be activated using PhysicsList FTFP_BERT.

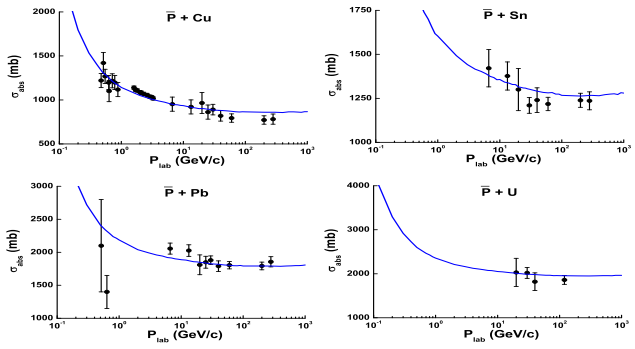

Figure 4: Absorption cross sections of anti-proton interactions with nuclei. The points are experimental data (see references in [11]), the lines are our calculations.

It is known that a projectile can have multiple intra-nuclear collisions in a target at high energies, or involves some nuclear nucleons at the fast stage of interactions. Distribution on the multiplicity of the

involved nucleon, ν, can be found applying the asymptotic Abramovsky-Gribov-Kancheli (AGK) cutting rules [12] to elastic scattering amplitude. For applications of the rules at low energies, we proposed [13] "finite energy corrections" to the rules, which decrease ν at low energies. These allowed to extend the FTF model to low energy domain.

In the first rough approximation, one can assume that an interaction of an anti-baryon with a nuclear nucleon is identical to the interaction with a free nucleon neglecting the binding energy of the nucleon, $\sim$ 10 MeV. Though, multiplicity of particles in hadron-nucleus interactions is larger than in hadron-nucleon ones. This is explained by the secondary particles cascading within a nucleus. The existing intra-nuclear cascade models have passed a long history of development and allow to simulate meson and baryon interactions with nuclei satisfactorily. Two of such models are present in Geant4 – the Bertini-like cascade model (BERT) and the binary cascade model (BIC) [14]. There is also a simplified model – the precompound model interface (PRECO), which only absorbs low energy particles ($E \leq 10$ MeV) produced by a high energy generator and located in a nuclear residual and ascribes them to the residual nuclei. The binary cascade model and the precompound model can be easily coupled with the FTF model. Therefore, we use in our following calculations two combinations of the models: FTF+BIC and FTF+PRECO[4]. FTFP demonstrates properties of interactions without intra-nuclear cascading. FTFB shows effects of the all cascading processes.

As seen in Fig. 5, FTFB describes the general properties of anti-proton-nucleus interactions, qualitatively. FTFP gives low yields of protons and neutrons. Thus, accounting of the particle cascading is very important for a correct simulation of the reactions.

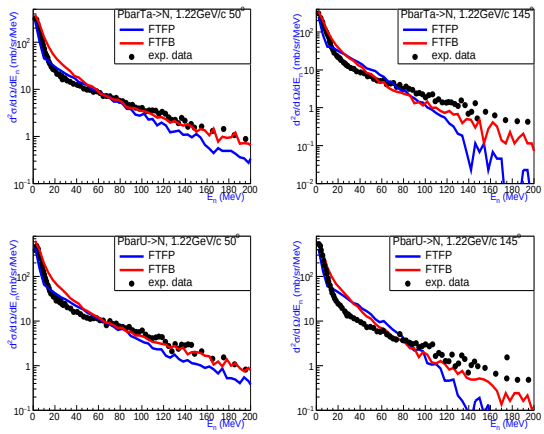

Figure 5: Neutron distributions on kinematical variables in anti-proton-nucleus interactions at P_{lab}=1.22 GeV/c. The points are experimental data [15]. The lines are our calculations. The red and blue lines are calculations with FTFB and FTFP, respectively.

4 Strange particle production

One of the aims of the PANDA experiment is a study of properties of hyper nuclei. It is planned that hyperons will be produced at interactions of anti-proton with hydrogen or nuclear target and will be absorbed by another nucleus forming a hyper nucleus. To reach the aim, it is needed to estimate multiplicity of hyperons and correctly reproduce their kinematical characteristics. Thus, we calculated with the FTF model average multiplicities of Λ-hyperons and K^0_S- mesons in anti-proton-proton interactions and presented them in Fig. 6. As seen, the model correctly reproduces the multiplicities below 10 GeV/c. At higher energies, the experimental data scatter too strongly, and it is complicated to draw a solid conclusion. The FTF model can also predict production of $\Sigma^{\pm\ 0}-$ and $\Xi^{0-}-$ hyperons, as well as their anti-particles.

Λ-hyperons are mainly produced in the process of Fig. 1b at a creation of $s\bar{s}$ quark's pair in a diquark-anti-diquark string. The analogous pair production takes place in the process of Fig. 1e. It is responsible

[4]These combinations are denoted as FTFB and FTFP, respectively.

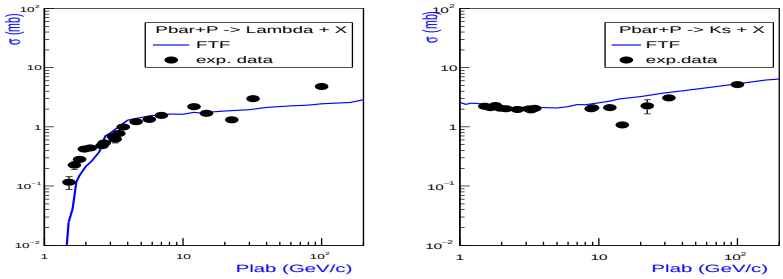

Figure 6: Average multiplicities of Λ-hyperons and K^0_S mesons as functions of projectile momentum. The points are experimental data, the lines are the FTF model calculations.

for creation of K^+K^- and K^0K^0 pairs at low energies. At high energies, the bottom processes of Fig. 1 start to dominate, which lead to slow increase of the strange particle multiplicities. Distributions of the strange particles on kinematical variables are very important for experiments. Calculated rapidity distributions of Λ-hyperons and K^0_S mesons in $\bar{p}p$ interactions at momenta 3.6, 12 and 100 GeV/c are presented in Fig. 7. As seen, there is a reasonable agreement with the experimental data.

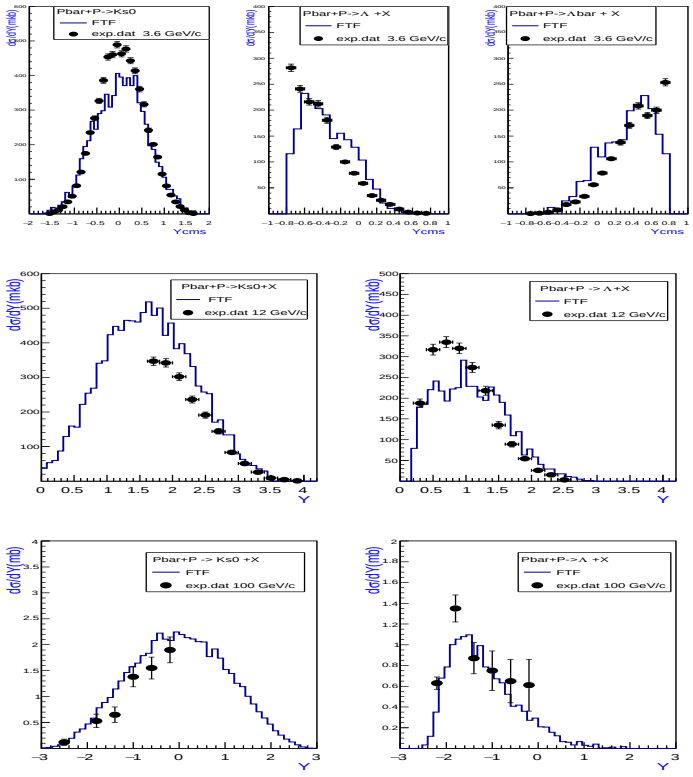

Figure 7: Rapidity distributions of Λ-hyperons and K^0_S mesons at P_{lab} = 3.6, 12 and 100 GeV/c. The points are experimental data, the lines are the FTF model calculations.

Λ and $\bar{\Lambda}$ productions in target and projectile fragmentation regions are connected with the processes $\bar{p}+p \to \bar{\Lambda}+\Lambda$ at low energies. At high energies, the processes can be $\bar{p}+p \to \bar{\Lambda}+K^0+p+m\ \pi$. As seen, K^0 mesons are mainly produced in the central region. It is natural at high energies. At low energies, K^0 mesons can be created in the processes $\bar{p}+p \to \bar{\Lambda}+K^0+n$ or $\bar{p}+p \to \bar{p}+K^0+\bar{K}^0+p$.

In Fig. 8, we present properties of $\bar{p}$+Xe interactions at 200 GeV/c. As seen, the FTF model describes general features of strange particle production in $\bar{p}+A$ collisions. This takes place also at lower energies.

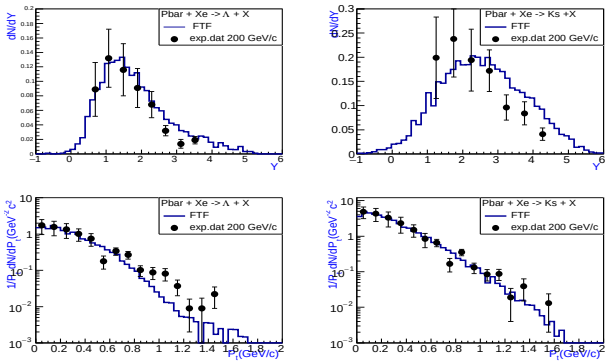

Figure 8: Rapidity and P_T^2 distributions of Λ-hyperons and K_S^0 mesons in $\bar{p} + Xe$ interactions at 200 GeV/c. The points are experimental data, the lines are the FTF model calculations.

5 Conclusion

The Dual Parton Model is implemented in the FTF model of Geant4 toolkit for simulations of anti-proton-proton and anti-proton-nucleus interactions. The model reproduces general features of the anti-proton interactions with nucleons and nuclei starting from annihilation at rest up to $\sim$ 1000 GeV/c.

6 Acknowledgements

The authors are thankful to heterogeneous computing team of LIT JINR (HybriLIT) for support of our calculations.

References

[1] S. Agostinelli (Geant4 Collaboration), *Nucl. Instrum. Methods A* **506** (2003) 250; J. Allison (Geant4 Collaboration), *IEEE Trans. Nucl. Sci.* **53** (2006) 270; J. Allison (Geant4 Collaboration), *Nucl. Instrum. Methods A* **835** (2016) 186.

[2] A. Capella, U. Sukhatme, C-I Tan, J. Tran Thanh Van, *Phys. Rept.* **236** (1994) 225; A.B. Kaidalov and K.A. Ter-Martirosian, *Phys. Lett. B* **117** (1982) 247.

[3] R.J. Glauber *Lectures in Theoretical Physics* v. **1**, Intersci. Publishers, N.Y., 1959;

[4] V.Franco *Phys. Rev.* **175** (1968) 1376;

[5] W.Czyz and L.C.Maximon *Ann. of Phys. (N.Y.)* **52** (1969) 59.

[6] V.V. Uzhinsky and A.S. Galoyan *arXive:0212369* [hep-ph] (2012).

[7] A.Galoian and V.Uzhinsky *AIP Conf. Proc.* **796** (2005) 79.

[8] A. Galoian, A. Ribon and V.Uzhinsky *PoS BaldinISHEPPXXII* (2015) 049.

[9] V. Franco and R.J. Glauber *Phys. Rev.* **142** (1966) 1195.

[10] O.D. Dalkarov and V.A. Karmanov *Nucl. Phys. A* **445** (1985) 579.

[11] V. Uzhinsky, J. Apostolakis, A. Galoyan et al. *Phys. Lett.B* **705** (2011) 235.

[12] V.A. Abramovsky, V.N. Gribov and O.V. Kancheli *Sov. J. Nucl. Phys.* **18** (1974) 308 (*Yad. Fiz.* **18** (1973) 595).

[13] A. Galoyan and V.Uzhinsky *Hyperfine Interact.* **215** (2013) 69.

[14] G. Folger, V.N. Ivanchenko and J.P. Wellisch *Eur. Phys. J. A* **21** (2004) 407.

[15] P.L.McGaughey et al. *Phys. Rev. Lett.* **56** (1986) 2156; H.J. Bersch et al. *Zeit. fur Phys. A* **292** (1979) 197.